



Cite this: *Chem. Sci.*, 2025, **16**, 4860

All publication charges for this article have been paid for by the Royal Society of Chemistry

Chemosel ective and laser cleavable probes for *in situ* protein lipoylation detection by laser desorption/ionization mass spectrometry†

Qiuyao Du,^{ab} Xi Yu,^{ab} Ke Jia,^{ab} Yijiao Qu,^{ab} Jing Han,^{ab} Jiameng Sun,^{ab} Duo Shen,^c Huihui Liu^{ab} and Zongxiu Nie^{ab}  *^{ab}

Protein lipoylation is a post-translational modification (PTM) of great significance as the lipoylation sites have essential effects on the enzymatic activities of several protein complexes, which affect the biological metabolic pathways and are further related to some diseases, such as cancer and Alzheimer's disease. While proteomic identification of lipoylated proteins has been studied, *in situ* profiling of protein lipoylation with high sensitivity remains challenging. Herein, we developed a strategy for *in situ* analysis of protein lipoylation by laser desorption/ionization-mass spectrometry (LDI-MS). In this study, a chemoselective butyraldehyde probe (BAP) was used to label the lipoylated proteins, and then linked with laser cleavable probe modified gold nanoparticles (AuNPs) through click chemistry. Triphenylmethyl mercaptan was used as mass tags (MTs) for the tertiary carbocations released under laser (355 nm) irradiation, which reflected the presence of protein lipoylation. Based on this strategy, a relative quantitative analysis of protein lipoylation on different cell lines was performed, and the distribution of lipoylated proteins in tissues was revealed by MS imaging (MSI). This novel approach used chemical modification to achieve signal amplification and overcome the low ionization efficiency and complicated mass spectra of standard protein analysis. This approach exhibits promise for uncovering biological processes and application in the diagnosis of related diseases.

Received 19th August 2024
Accepted 23rd January 2025

DOI: 10.1039/d4sc05553e
rsc.li/chemical-science

Introduction

Protein lipoylation is an essential post-translational modification (PTM) in organisms, formed by the covalent bonding of lipoic acid (LA) to particular lysine residues.^{1,2} Lipoylation sites are required for the enzymatic activities of several protein complexes in core metabolic pathway reactions, such as pyruvate dehydrogenase (PDH), α -ketoglutarate dehydrogenase (KDH), branched-chain α -ketoacid dehydrogenase (BCKDH), and glycine cleavage (GCV).³ These proteins are involved in various metabolic pathways, including glycolysis, the tricarboxylic acid (TCA) cycle, fatty acid metabolism, reactive oxygen species metabolism, amino acid catabolic processes, etc.^{4–6} For example, PDH can catalyze the decarboxylation of pyruvate in the TCA cycle to produce acetyl-CoA.⁷ Dihydrolipoamide *S*-acyltransferase (DLAT) is an essential component of the PDH

complex.⁸ Studies have shown that the binding of copper ions to lipoylated DLAT can lead to the oligomerization of proteins, thereby inducing cell death.⁹ Besides, dysregulation of protein lipoylation is associated with a variety of diseases, such as cancer, Alzheimer's disease, neonatal-onset epilepsy and variant non-ketotic hyperglycinemia.^{4,10–12} Therefore, the analysis of protein lipoylation is of vital importance to disease diagnosis and the understanding of relative biological processes.

Antibodies have been widely used for immunoprecipitating lipoylated proteins for proteomic identification by liquid chromatography-tandem mass spectrometry (LC-MS/MS).¹³ However, the binding affinity of antibodies against PTM moieties was not strong enough, which limited their applications.¹⁴ An alternative is chemoselective small-molecule probes that covalently conjugate with PTMs. Xing Chen *et al.* have developed a chemoselective ligation strategy, iodoacetamide-assisted lipoate-cyclooctyne ligation (iLCL), to chemically capture and enrich lipoylated proteins by using iodoacetamide and cyclooctyne.¹⁴ Chu Wang *et al.* developed a butyraldehyde probe (BAP) that enables direct labeling and enrichment of protein lipoylation in proteomes.¹⁵ However, these methods have tedious sample preparation procedures and lose the spatial distribution information of PTMs.¹⁶ Besides, they have strict requirements for the sensitivity of the mass spectrometer.

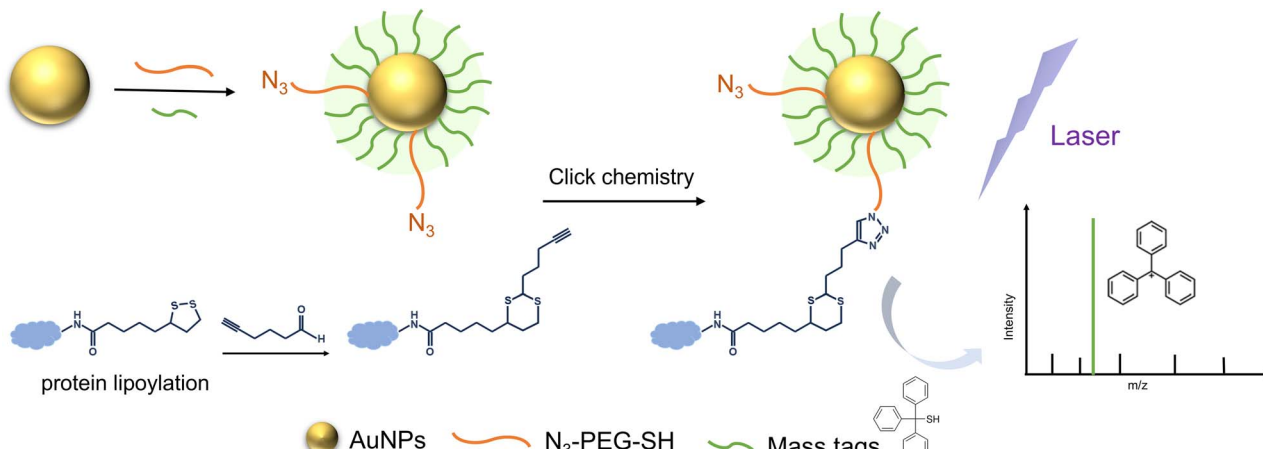
^aBeijing National Laboratory for Molecular Sciences, Key Laboratory of Analytical Chemistry for Living Biosystems, Institute of Chemistry, Chinese Academy of Sciences, Beijing 100190, China. E-mail: znie@iccas.ac.cn

^bUniversity of Chinese Academy of Sciences, Beijing 100049, China

^cAcademician Workstation, Jiangxi University of Chinese Medicine, Nanchang 330004, Jiangxi, China

† Electronic supplementary information (ESI) available: Experimental section and ESI figures. See DOI: <https://doi.org/10.1039/d4sc05553e>





Scheme 1 Strategy based on the chemoselective and laser cleavable probes for *in situ* protein lipoylation detection by LDI-MS.

Laser desorption/ionization-mass spectrometry (LDI-MS) has certain advantages in rapid and sensitive analysis, as well as obtaining *in situ* information of analytes.¹⁷ Bai and colleagues designed bifunctional cleavable probes for *in situ* multiplexed glycan detection and imaging by LDI-MS.¹⁸ Our research group used laser cleavable probes for *in situ* sialoglycoconjugate profiling and multiplexed glycan detection in single cells by LDI-MS.^{19,20} But until now, the research into *in situ*, rapid and sensitive analysis of lipoylation PTMs by LDI-MS has been lacking.

Herein, a strategy for *in situ* analysis of protein lipoylation by LDI-MS was proposed (Scheme 1). This extraction-free and sensitive method combined chemoselective small-molecule probes, click chemistry, and a signal amplification strategy based on gold nanoparticles (AuNPs) and laser cleavable mass tags.^{21–23} The BAP was synthesized for the labeling of protein lipoylation according to Wang's study. Azido-polyethylene glycol-thiol (N₃-PEG-SH) as the linking group connected the probe to the AuNPs covering triphenylmethyl mercaptan as mass tags (MTs) by click chemistry. Under laser (355 nm) irradiation, the carbon–sulfur (C–S) bond of MTs could be broken efficiently, and tertiary carbocations were released for the sensitive detection by LDI-MS. Although the combination of click chemistry with modified gold nanoparticles has been used in analytical chemistry, it has not been used for the analysis of post-translational modification of proteins as far as we know. Based on this strategy, we performed relative quantitative analysis of protein lipoylation on different cell lines.²⁴ Furthermore, MS imaging to provide the visible distribution of lipoylated proteins was also conducted. This novel approach provided mass spectrometric evidence of different expression levels of lipoylation, revealing the correlation with diseases. By combining various probes, it can also be used for other PTM analyses. Thus, this approach has potential for deciphering biological events and application in diseases diagnosis and therapeutic treatment.

Results and discussion

Synthesis and characterization of MTs/N₃@AuNPs

The BAP was synthesized for labeling lipoylation according to the previous study of Chu Wang *et al.*¹⁵ The alkyne handle of the

BAP could be conjugated with azido-functionalized AuNPs *via* copper(i)-catalyzed azide–alkyne cycloaddition (CuAAC), and the AuNPs were modified with triphenylmethyl mercaptan as MTs for releasing tertiary carbocations under laser irradiation to provide a high sensitivity for protein detection. N₃-PEG-SH (5000 Da) was used as the linker between the BAP and AuNPs for the azido terminal aimed for the click reaction with the alkyne handle of the BAP, and the sulphydryl terminal linked to the AuNPs. Triphenylmethyl mercaptan which had high efficiency in releasing triphenylmethyl cations under laser irradiation was chosen as the MS reporter grafted on the surface of AuNPs through the formation of Au–S bonds.¹⁹ Proportions of Au, N₃-PEG-SH and triphenylmethyl mercaptan were systematically optimized to obtain highly sensitive and reactive MTs/N₃@AuNPs. Transmission electron microscopy (TEM) measurements showed that the synthesized AuNPs had a diameter of approximately 15 nm, and MTs/N₃@AuNPs had a corona of 2 nm thickness (Fig. 1a and S1†).^{25,26} Ultraviolet-visible (UV-vis) absorption spectra corresponding to the MTs/N₃@AuNPs and the original AuNPs exhibited significant variation, suggesting that MTs/N₃@AuNPs were prepared successfully (Fig. 1b). N₃-PEG-SH and MTs were modified on AuNPs to form MTs/N₃@AuNPs which could produce characteristic mass signals with high intensity in LDI-MS without an additional matrix. The mass spectrum of MTs/N₃@AuNPs in positive ion mode showed a higher intensity of triphenylmethyl cations at *m/z* 243 than the signals of Au⁺, 2Au⁺ and 3Au⁺ at *m/z* 197, 394 and 591 (Fig. 1c). High mass resolution LDI-FTICR-MS results are shown in Fig. S2.† The MTs achieved signal amplification in this strategy, which facilitated that rapid identification even under complex matrices for the characteristic fragment ion would avoid signal interference from the sample background.

In situ detection of protein lipoylation in cells by LDI-MS

Human neuroblastoma (SK-N-SH) cells were chosen to verify *in situ* analysis of protein lipoylation. After 24 h of incubation and attachment, the cells were fixed with 4% paraformaldehyde (PFA) at 4 °C overnight, and penetrated with 0.2% Triton-X100 for 10 min. To exclude the “side reactions” between the BAP and



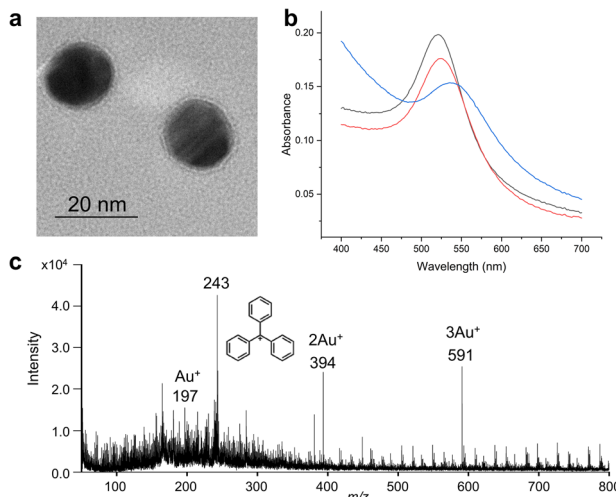


Fig. 1 Characterization of MTs/N₃@AuNPs. (a) Transmission electron microscopy (TEM) image of MTs/N₃@AuNPs. (b) Ultraviolet-visible (UV-vis) absorption spectra of bare AuNPs (black), N₃@AuNPs (red) and MTs/N₃@AuNPs (blue). (c) MS spectrum of MTs/N₃@AuNPs (*m/z* 243 represents the triphenylmethyl cation released from MTs; *m/z* 197, 394 and 591 represent the signal of Au).

cysteine, the cells were treated with 100 mM *N*-ethylmaleimide (NEM) 3 h for blocking protein thiol, and then incubated with 20 mM BAP and 10 mM tris(2-carboxyethyl)phosphine (TCEP) in an acidic buffer system (pH = 3) for 12 h at 37 °C.^{14,15} For comparison, cells without the BAP added and cells cultured with the BAP for 5 min were set as control groups to exclude the nonspecific adsorption of cells. The cells were washed with phosphate buffered saline (PBS) in each step. After washing to remove the excess BAP, 500 μL of reaction solution (0.2 mM tris [(1-benzyl-1*H*-1,2,3-triazol-4-yl)methyl]amine (TBA), 0.2 mM TCEP, 1.0 mM CuSO₄, and 2.0 mM sodium ascorbate in MTs/N₃@AuNPs) was added for the click reaction for 6 h. Finally, the completely washed cells (1% Tween-20 and PBS) were then scraped and directly spotted on the target plate for LDI-MS detection. The results showed that the signal of MTs was obtained at *m/z* 243, while in the control groups no signal at *m/z* 243 was observed (Fig. 2 and S3a†). To confirm the conjugation of the BAP to the cells, Cyanine5-azide (Cy5-azide) was employed for the imaging of the BAP under a confocal laser scan microscope (CLSM). Confocal imaging results showed that the experimental group exhibited strong fluorescence signals of the cells after incubation with Cy5-azide and the click reaction reagent while no obvious signal was observed in the control groups (Fig. S3b†). To further verify the interaction between the BAP and lipoylation cells attributed to the specific binding, a lipoic acid (LA) inhibition experiment was conducted. The BAP was pre-incubated with LA, followed by incubation with cells. The BAP-MTs/N₃@AuNPs strategy was conducted with LDI-MS analysis, and no obvious MTs signal was detected (Fig. S4†). These results demonstrated that the BAP specifically labeled protein lipoylation in cells, and the BAP-MTs/N₃@AuNPs strategy is effective for protein lipoylation analysis by LDI-MS.

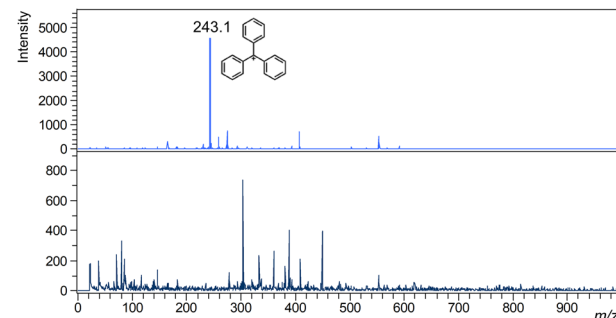


Fig. 2 *In situ* detection of protein lipoylation in cells. MS spectra obtained using the BAP-MTs/N₃@AuNPs strategy for protein lipoylation analysis by LDI-MS with the BAP incubated for 12 h (top) and without the BAP added (bottom).

Quantitative analysis of protein lipoylation in different cells

Quantitative information of protein lipoylation is crucial to understand the potential molecular mechanisms of lipoylation-related diseases and biological processes. The relative quantification of protein lipoylation was performed by evaluating the relative intensities of MTs and internal standard (IS). Tris(4-methoxyphenyl)methanol was chosen as the IS for its similar structure and ionization performance to MTs. The characteristic MS signal corresponding to the IS was a tertiary carbocation at *m/z* 333 which was generated under laser irradiation by LDI-MS. The IS with a concentration of 25 μM and a series of concentrations of MTs were mixed and measured to draw the standard curve (Fig. 3a). The repetitive assays were found to exhibit desired reproducibility, implying the use of an IS based procedure offering the possibility of lipoylation protein quantification. The limit of detection for MTs is 0.25 μM. Relative quantitative analysis was applied to three different cell lines including SK-N-SH cells, Michigan cancer foundation-7 (MCF-7) cells and human embryonic kidney 293 (HEK 293) cells. After culturing for 24 h, the average counts of the three different cell lines were 3.36 × 10⁶, 3.52 × 10⁶, and 3.04 × 10⁶ per dish, respectively. The representative mass spectra of the three cell lines are shown in Fig. 3b. The concentrations of MTs were calculated according to the standard curve. Compared with the number of cells, the average relative concentration of MTs for each cell of the three different cell lines was approximately 1.00,

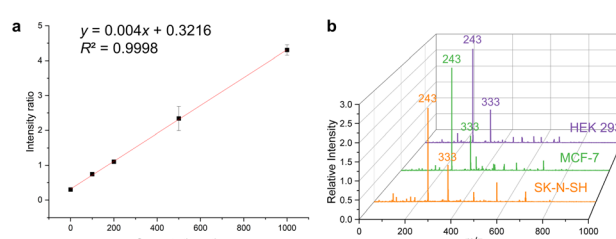


Fig. 3 Quantitative analysis of protein lipoylation in different cells. (a) Calibration curve of MTs (x-axis, concentration ratio of MTs to IS; y-axis, intensity ratio of *m/z* 243 against *m/z* 333). (b) Representative mass spectra of three cell lines with the BAP-MTs/N₃@AuNPs strategy by LDI-MS.

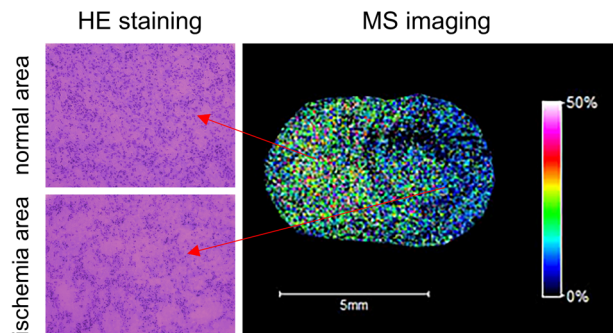


Fig. 4 Hematoxylin and eosin (HE) staining of the brain tissue section from the neonatal rat model of hypoxic-ischemic encephalopathy (HIE) and MS image of protein lipoylation in the ischemic region and contralateral region.

1.06, and 1.22, respectively. The results implied the heterogeneity in protein lipoylation content among different cell lines, and indicated the lower expression of protein lipoylation in cancer cells than in normal cells to a certain extent. This might be related to the “Warburg effect” of cancer cells for the tricarboxylic acid (TCA) cycle disturbance.²⁷ The mechanism for the cell-type-specific difference in protein lipoylation remains to be investigated.

MS imaging of fresh tissues

While the visible distribution of protein lipoylation in tissues by MS imaging (MSI) is vital for the knowledge of related biological processes, direct MSI analysis is challenging. Here, we applied our *in situ* detection strategy based on BAP-MTs/N₃@AuNPs to convert protein lipoylation into the MT signal, and achieved the protein lipoylation MSI analysis.^{28,29} We evaluated the protein lipoylation in the brain tissues of neonatal rats with hypoxic-ischemic encephalopathy (HIE). The establishment of the neonatal rat model of HIE was carried out as in our previous work.³⁰ The hematoxylin and eosin (HE) staining of the tissue section is shown in Fig. 4. The left hemisphere of the rat brain is the normal area, and the right hemisphere is the ischemia area. As shown in Fig. 4, the MSI results indicated that the protein lipoylation level in the ischemia area was lower than that in the normal area. This may be related to disturbances in certain biological processes and functions of protein lipoylation in the ischemic region. We also applied this BAP-MTs/N₃@AuNPs strategy to human brain glioma tissue and obtained the visible distribution of protein lipoylation (Fig. S5†). Unfortunately, a small amount of normal brain tissue we obtained was washed out during the pretreatment process due to the high lipid content and could not be compared with cancer tissue. The results indicated the capability of this method to detect the distribution and alteration of protein lipoylation.

Conclusions

In conclusion, a high sensitivity and low interference approach based on LDI-MS was developed for *in situ* detection of protein

lipoylation. A chemoselective BAP probe was used to label lipoylated proteins, and was linked with laser cleavable probe modified AuNPs. Thus, the detection of protein lipoylation could be conducted by replacing the signal of MTs for it under laser (355 nm) irradiation. Based on this strategy, the low ionization efficiency and complicated mass spectra of protein analysis were overcome by signal amplification without the addition of a matrix. Furthermore, relative quantitative analysis of protein lipoylation on different cell lines was performed, and the visible distribution of lipoylated proteins in tissues was revealed by MSI. This strategy can also be used for other PTM analyses by combining various labeling probes. This extraction-free and sensitive method provides mass spectrometric evidence of different expression levels of lipoylation, and exhibits promise for uncovering the biological events and application in disease diagnosis and therapeutic treatment.

Ethical statement

Human glioma tissue was obtained during surgery. All experiments were performed in accordance with the Measures for the Ethical Review of Biomedical Research Involving Human Subjects issued by the National Health and Family Planning Commission of The People's Republic of China, and approved by the Medical Ethics Committee of Beijing Tiantan Hospital Affiliated to Capital Medical University. Informed consent was obtained from human participants of this study.

Data availability

The data are available in the ESI† or upon request from the authors.

Author contributions

Zongxiu Nie: formulation and evolution of overarching research goals and aims. Qiuyao Du: creation and presentation of the published work. Jiameng Sun and Yijiao Qu: provision of study materials, reagents and materials. Xi Yu and Ke Jia: application of statistical, mathematical and computational techniques. Huihui Liu and Duo Shen: development and design of methodology. Jing Han: management and coordination responsibility for the research activity planning and execution.

Conflicts of interest

There are no conflicts to declare.

Acknowledgements

We are grateful for the financial support from the National Natural Sciences Foundation of China (grant no. 22334007, 22274160, and 22304175) and the Chinese Academy of Sciences.

Notes and references

1 R. N. Perham, Swinging arms and swinging domains in multifunctional enzymes: Catalytic machines for multistep reactions, *Annu. Rev. Biochem.*, 2000, **69**, 961–1004.

2 Y. S. Xie, L. F. Chen, R. Wang, J. G. Wang, J. Y. Li, W. Xu, Y. X. Li, S. Q. Yao, L. Zhang, Q. Hao and H. Y. Sun, Chemical Probes Reveal Sirt2's New Function as a Robust "Eraser" of Lysine Lipoylation, *J. Am. Chem. Soc.*, 2019, **141**, 18428–18436.

3 E. A. Rowland, C. K. Snowden and I. M. Cristea, Protein lipoylation: an evolutionarily conserved metabolic regulator of health and disease, *Curr. Opin. Chem. Biol.*, 2018, **42**, 76–85.

4 J. M. Blouin, G. Penot, M. Collinet, M. Nacfer, C. Forest, P. Laurent-Puig, X. Coumoul, R. Barouki, C. Benelli and S. Bortoli, Butyrate elicits a metabolic switch in human colon cancer cells by targeting the pyruvate dehydrogenase complex, *Int. J. Cancer*, 2011, **128**, 2591–2601.

5 J. Kluza, P. Corazao-Rozas, Y. Touil, M. Jendoubi, C. Maire, P. Guerreschi, A. Jonneaux, C. Ballot, S. Balayssac, S. Valable, A. Corroyer-Dulmont, M. Bernaudin, M. Malet-Martino, E. M. de Lassalle, P. Maboudou, P. Formstecher, R. Polakowska, L. Mortier and P. Marchetti, Inactivation of the HIF-1 α /PDK3 Signaling Axis Drives Melanoma toward Mitochondrial Oxidative Metabolism and Potentiates the Therapeutic Activity of Pro-Oxidants, *Cancer Res.*, 2012, **72**, 5035–5047.

6 R. A. Harris, B. Zhang, G. W. Goodwin, M. J. Kuntz, Y. Shimomura, P. Rougraff, P. Dexter, Y. Zhao, R. Gibson and D. W. Crabb, Regulation of the branched-chain alpha-ketoacid dehydrogenase and elucidation of a molecular basis for maple syrup urine disease, *Adv. Enzyme Regul.*, 1990, **30**, 245.

7 R. A. Mathias, T. M. Greco, A. Oberstein, H. G. Budayeva, R. Chakrabarti, E. A. Rowland, Y. B. Kang, T. Shenk and I. M. Cristea, Sirtuin 4 Is a Lipoamidase Regulating Pyruvate Dehydrogenase Complex Activity, *Cell*, 2014, **159**, 1615–1625.

8 W. Q. Liu, W. R. Lin, L. Yan, W. H. Xu and J. Yang, Copper homeostasis and cuproptosis in cancer immunity and therapy, *Immunol. Rev.*, 2024, **321**, 211–227.

9 P. Tsvetkov, S. Coy, B. Petrova, M. Dreishpoon, A. Verma, M. Abdusamad, J. Rossen, L. Joesch-Cohen, R. Humeidi, R. D. Spangler, J. K. Eaton, E. Frenkel, M. Kocak, S. M. Corsello, S. Lutsenko, N. Kanarek, S. Santagata and T. R. Golub, Copper induces cell death by targeting lipoylated TCA cycle proteins, *Science*, 2022, **375**, 1254.

10 C. B. Pocernich and D. A. Butterfield, Acrolein inhibits NADH-linked mitochondrial enzyme activity: implications for Alzheimer's disease, *Neurotoxic. Res.*, 2003, **5**, 515–519.

11 J. A. Mayr, F. A. Zimmermann, C. Fauth, C. Bergheim, D. Meierhofer, D. Radmayr, J. Zschocke, J. Koch and W. Sperl, Lipoic Acid Synthetase Deficiency Causes Neonatal-Onset Epilepsy, Defective Mitochondrial Energy Metabolism, and Glycine Elevation, *Am. J. Hum. Genet.*, 2011, **89**, 792–797.

12 P. R. Baker, M. W. Friederich, M. A. Swanson, T. Shaikh, K. Bhattacharya, G. H. Scharer, J. Aicher, G. Creadon-Swindell, E. Geiger, K. N. MacLean, W. T. Lee, C. Deshpande, M. L. Freckmann, L. Y. Shih, M. Wasserstein, M. B. Rasmussen, A. M. Lund, P. Procopis, J. M. Cameron, B. H. Robinson, G. K. Brown, R. M. Brown, A. G. Compton, C. L. Dieckmann, R. Collard, C. R. Coughlin, E. Spector, M. F. Wempe and J. L. K. Van Hove, Variant non ketotic hyperglycinemia is caused by mutations in LIAS, BOLA3 and the novel gene GLRX5, *Brain*, 2014, **137**, 366–379.

13 K. Tajima, K. Ikeda, H. Y. Chang, C. H. Chang, T. Yoneshiro, Y. Oguri, H. Jun, J. Wu, Y. Ishihama and S. Kajimura, Mitochondrial lipoylation integrates age-associated decline in brown fat thermogenesis, *Nat. Metab.*, 2019, **1**, 886–898.

14 Q. Tang, Y. L. Guo, L. Y. Meng and X. Chen, Chemical Tagging of Protein Lipoylation, *Angew. Chem., Int. Ed.*, 2021, **60**, 4028–4033.

15 S. C. Lai, Y. Chen, F. Yang, W. D. Xiao, Y. Liu and C. Wang, Quantitative Site-Specific Chemoproteomic Profiling of Protein Lipoylation, *J. Am. Chem. Soc.*, 2022, **144**, 10320–10329.

16 Y. Zhai, L. Chen, Q. Zhao, Z. H. Zheng, Z. N. Chen, H. J. Bian, X. Yang, H. Y. Lu, P. Lin, X. Chen, R. Chen, H. Y. Sun, L. N. Fan, K. Zhang, B. Wang, X. X. Sun, Z. Feng, Y. M. Zhu, J. S. Zhou, S. R. Chen, T. Zhang, S. Y. Chen, J. J. Chen, K. Zhang, Y. Wang, Y. Chang, R. Zhang, B. Zhang, L. J. Wang, X. M. Li, Q. He, X. M. Yang, G. Nan, R. H. Xie, L. Yang, J. H. Yang and P. Zhu, Cysteine carboxylation generates neoantigens to induce HLA-restricted autoimmunity, *Science*, 2023, **379**, 1104.

17 X. C. Lin, X. N. Wang, L. Liu, Q. Wen, R. Q. Yu and J. H. Jiang, Surface Enhanced Laser Desorption Ionization of Phospholipids on Gold Nanoparticles for Mass Spectrometric Immunoassay, *Anal. Chem.*, 2016, **88**, 9881–9884.

18 W. Ma, S. T. Xu, H. G. Nie, B. Y. Hu, Y. Bai and H. W. Liu, Bifunctional cleavable probes for in situ multiplexed glycan detection and imaging using mass spectrometry, *Chem. Sci.*, 2019, **10**, 2320–2325.

19 J. Sun, H. H. Liu, L. P. Zhan, C. Q. Xiong, X. Huang, J. J. Xue and Z. X. Nie, Laser Cleavable Probes-Based Cell Surface Engineering for in Situ Sialoglycoconjugates Profiling by Laser Desorption/Ionization Mass Spectrometry, *Anal. Chem.*, 2018, **90**, 6397–6402.

20 J. Han, X. Huang, H. H. Liu, J. Y. Wang, C. Q. Xiong and Z. X. Nie, Laser cleavable probes for in situ multiplexed glycan detection by single cell mass spectrometry, *Chem. Sci.*, 2020, **11**, 1176.

21 Q. X. Nie, X. Luo, K. Wang, Y. Ding, S. M. Jia, Q. X. Zhao, M. Li, J. X. Zhang, Y. Y. Zhuo, J. Lin, C. H. Guo, Z. W. Zhang, H. Y. Liu, G. Y. Zeng, J. You, L. L. Sun, H. Lu, M. Ma, Y. X. Jia, M. H. Zheng, Y. L. Pang, J. Qiao and C. T. Jiang, Gut symbionts alleviate MASH through



a secondary bile acid biosynthetic pathway, *Cell*, 2024, **187**, 2717–2734.

22 J. J. Hu, F. Liu, Y. L. Chen, G. Q. Shangguan and H. X. Ju, Mass Spectrometric Biosensing: A Powerful Approach for Multiplexed Analysis of Clinical Biomolecules, *ACS Sens.*, 2021, **6**, 3517–3535.

23 R. H. Chen, Y. P. Xiao, H. T. Liu, L. Fang, J. H. Liu, X. L. Ruan, B. W. Chen and T. G. Luan, Lab-on-Membrane Platform Coupled with Paper Spray Ionization for Analysis of Prostate-Specific Antigen in Clinical Settings, *Anal. Chem.*, 2020, **92**, 13298–13304.

24 Y. N. Wang, K. Zhang, X. D. Huang, L. Qiao and B. H. Liu, Mass Spectrometry Imaging of Mass Tag Immunoassay Enables the Quantitative Profiling of Biomarkers from Dozens of Exosomes, *Anal. Chem.*, 2021, **93**, 709–714.

25 X. H. Ji, X. N. Song, J. Li, Y. B. Bai, W. S. Yang and X. G. Peng, Size control of gold nanocrystals in citrate reduction: The third role of citrate, *J. Am. Chem. Soc.*, 2007, **129**, 13939–13948.

26 S. D. Perrault and W. C. W. Chan, Synthesis and Surface Modification of Highly Monodispersed, Spherical Gold Nanoparticles of 50–200 nm, *J. Am. Chem. Soc.*, 2009, **131**, 17042.

27 M. G. V. Heiden, L. C. Cantley and C. B. Thompson, Understanding the Warburg Effect: The Metabolic Requirements of Cell Proliferation, *Science*, 2009, **324**, 1029–1033.

28 J. L. Norris and R. M. Caprioli, Analysis of Tissue Specimens by Matrix-Assisted Laser Desorption/Ionization Imaging Mass Spectrometry in Biological and Clinical Research, *Chem. Rev.*, 2013, **113**, 2309–2342.

29 R. J. A. Goodwin, S. R. Pennington and A. R. Pitt, Protein and peptides in pictures: Imaging with MALDI mass spectrometry, *Proteomics*, 2008, **8**, 3785–3800.

30 H. H. Liu, T. Xie, J. Y. Wang, X. Wang, J. Han, Z. H. Huang, L. X. Jiang and Z. X. Nie, In situ analysis of metabolic changes under hypoxic-ischemic encephalopathy via MALDI mass spectrometry imaging, *Talanta*, 2024, **268**, 125306.

